GEOPHYSICS, VOL. 60, NO. 2 (MARCH-APRIL 1995); P. 399-407, 4 FIGS.

Interpolation of potential-field data by equivalent layer and minimum curvature: A comparative analysis

Carlos A. Mendonça* and João B. C. Silva‡

ABSTRACT

Interpolation using only the observations at discrete points is an ill-posed problem because it admits infinite solutions. Usually, to reduce ambiguity, a priori information about the sample function is introduced. Current interpolation methods in mineral exploration introduce only the constraints of continuity and smoothness of the interpolating function. In interpolating potential-field anomalies, the constraint that the sampled function is harmonic may be introduced by the equivalent-layer method (ELM).

We compare the performance of the ELM and the minimum curvature method (MCM) in interpolating potential-field anomalies by applying these methods to synthetic magnetic data simulating an aeromagnetic survey. In the case the anomaly flanks and peak are undersampled, the ELM performs better than the MCM in recovering the anomaly gradients and peak. In the case of elongated linear anomalies, the ELM recovers the exact linear pattern, but the MCM introduces spurious oscillations in the linear pattern. Also, the ELM is able to reduce the data from a survey flown at different heights to a common level. In contrast, the MCM, being a 2-D interpolation method, cannot account for variations in the vertical coordinates of the observation points.

INTRODUCTION

Several interpretation methods in potential-field data require that the anomaly be sampled at regular intervals, as for example, in processing and interpretation using the fast Fourier transform (Gunn, 1975; Oldenburg, 1975). Linear transformations using the equivalent layer also become much more efficient when the data are regularly spaced (Leão and Silva, 1989). Acquiring regularly spaced data, however, is operationally difficult, so it is easier to produce a regular grid of interpolated values from the original irregularly sampled data.

Interpolation, using *only* the measured data, is an ill-posed problem because it admits infinite solutions, that is, any function passing through the observed data is a solution to the interpolation problem. As a result, to transform this ill-posed problem into a well-posed problem, it is usual to introduce a priori information about the behavior of the sampled function. The a priori information usually considered are the continuity and the smoothness of the sampled function. In addition, it is assumed that the average distance among adjacent observations is close to the Nyquist interval so that no oscillations are expected to occur between any two adjacent observations. Among the interpolation methods using this kind of a priori information are the weighted average, polynomial fitting, and splines.

In the weighted average method (Franke, 1980), the interpolated field at point P is taken as the weighted average of the n observations closest to P. The weight associated to the ith observation is a power γ of the inverse of the distance between the position of this observation and the position of point P. Depending on the values assigned to γ and n, different methods are obtained (La Porte, 1962; Shepard, 1969). The greater the values of γ and n, the smoother the interpolating function.

In the polynomial fitting method, the interpolating function is a polynomial of order p whose coefficients are computed by solving a linear system of equations. The interpolated values at any point may be obtained by evaluating the polynomial at that point. The smaller the polynomial order p, the smoother the interpolating function. When the total number of observation N is large, the polynomial order may be high to fit all observations. This may produce undesirable oscillations between adjacent observations. To minimize this effect, the polynomial is fitted using a subset of

Manuscript received by the Editor March 28, 1994; revised manuscript received March 28, 1994.
*Department Geofísica, USP, R. do Matão 1226, Caixa, Postal 05508-900, São Paulo—S.P.—Brazil.
‡CG—UFPA—Caixa, Postal 1611, 66017—900—Belém—Pará—Brazil.

$N1$ ($N1 < N$) points that are closest to the interpolating point (Braile, 1978). In both methods, weighted average and polynomial fitting, the continuity of the interpolating function is guaranteed by the continuity of the inverse of distance and polynomial functions, respectively.

Interpolating by spline functions comprises a wide class of methods. This kind of function presents minimum curvature in the x-y plane and is the solution of the biharmonic equation with boundary conditions of continuity of the function and its first and second derivatives (Gonzalez-Casanova and Alvarez, 1985). Two-dimensional splines were developed by Briggs (1974) who discretized the curvature functional using the finite-differences method. The criterion of minimum curvature leads to a linear system of equations whose associated matrix is sparse and is solved by the iterative method of Gauss-Seidel.

In interpolating potential-field data, the important information that the interpolating function must satisfy Laplace's equation is not incorporated by the above mentioned methods. There are only two methods in the literature that use this information. The first one is the collocation method (Moritz, 1977, 1978) which has been used to represent the earth's gravity anomalous potential, and to a lesser extent, to exploration problems (Morrison and Douglas, 1984). The second one is the equivalent layer method (Dampney, 1969) which has been used extensively in processing potential-field anomalies (Bott and Ingles, 1972; Emilia, 1973; Mayhew et al., 1980; Leão and Silva, 1989, for example), but was applied only recently to interpolation problems (Cordell, 1992; Mendonça and Silva, 1994).

The purpose of this paper is to compare the performance of the equivalent layer technique as an interpolation method with the minimum curvature method of Briggs (1974) which is one of the most popular interpolation methods. Because the equivalent-layer method (ELM) assumes that the interpolating function, besides being continuous and smooth is also harmonic, it has a better performance than the minimum curvature method (MCM) in recovering undersampled anomaly amplitudes and gradients. The comparison is performed using synthetic data only because the true interpolated values must be known.

METHODOLOGY

Minimum curvature method

This method has been thoroughly described by Briggs (1974). We indicate here only the principal points. Briggs (1974) pointed out that the optimum properties of the spline fit can be obtained by solving the differential equation equivalent to a third-order spline:

$$\left(\frac{\partial^2}{\partial x^2}+\frac{\partial^2}{\partial y^2}\right)\left(\frac{\partial^2 u}{\partial x^2}+\frac{\partial^2 u}{\partial y^2}\right)=0, \tag{1}$$

where u is the interpolating function. The boundary conditions impose that $u(x_n, y_n) = g_n$, the nth observation, and that between the edge of the interpolating region and the observations, the interpolating function will tend to a plane as the interpolating region becomes larger.

Briggs (1974) showed that a function $u(x, y)$ that minimizes the total squared curvature:

$$C(u)=\int\int\left(\frac{\partial^2 u}{\partial x^2}+\frac{\partial^2 u}{\partial y^2}\right)^2 dx\,dy, \tag{2}$$

obeys equation (1), and conversely, if a function u obeys equation (1) it minimizes $C(u)$.

By expressing the discrete total squared curvature as,

$$C=\sum_{i=1}^{I}\sum_{j=1}^{J}(u_{i+1,j}+u_{i-1,j}+u_{i,j+1}+u_{i,j-1}-4u_{i,j})^2/h^2, \tag{3}$$

where h is the grid spacing in both the x- and y-directions, and $u_{i,j}$ is the interpolated value at grid point (i, j), we obtain the following system of linear equations from the necessary conditions to minimize C:

$$u_{i+2,j}+u_{i,j+2}+u_{i-2,j}+u_{i,j-2}+2(u_{i+1,j+1}+u_{i-1,j+1}+u_{i+1,j-1}+u_{i-1,j-1})-8(u_{i+1,j}+u_{i-1,j}+u_{i,j-1}+u_{i,j+1})+20u_{i,j}=0,\ i=1,\ldots,I,\ j=1,\ldots,J, \tag{4}$$

for observation points coinciding with a grid point. For observation points not on a grid point, an approximate expression for $\partial^2 u/\partial x^2 + \partial^2 u/\partial y^2$ at a given point (x_0, y_0) is obtained by expanding u in Taylor's series around (x_0, y_0) and using equation (3). Another system of equations is then obtained from the necessary conditions to minimize C. Solving the above mentioned linear systems of equations leads to the interpolated values $u_{i,j}$, $i = 1 \ldots I$, $j = 1 \ldots J$.

Equivalent layer method

By the equivalent layer principle, the potential-field observations can be written as

$$\mathbf{d}=\underline{\mathbf{G}}\mathbf{p}, \tag{5}$$

where $\mathbf{d}$ is a vector with N observations, $\mathbf{p}$ is a vector with M unknown intensities of the equivalent sources, and $\underline{\mathbf{G}}$ is an $N \times M$ kernel matrix that maps the sources to data. The element $g_{n,m}$ of $\underline{\mathbf{G}}$ is written as

$$g_{n,m}=g(x_n-x_m, y_n-y_m, z_n-h), \tag{6}$$

and represents, at the nth observation location (x_n, y_n, z_n), a quantity proportional to the effect of the mth equivalent source situated at (x_m, y_m, h).

We formulate the equivalent layer problem given in equation (5) in an underdetermined way, by assuming a number of equivalent sources greater than the number of observations. As compared to an overdetermined formulation, this formulation yields smaller residuals between the observations and their representations in equation (5) which is a very important requirement for an interpolation method.

Formulated as an underdetermined problem, equation (5) does not have a unique solution. Therefore, we look for the solution that has minimum Euclidean norm. As the data are corrupted with noise, we use a damping factor, $\lambda > 0$ (Silva, 1986) to obtain the estimator $\hat{\mathbf{p}}$ as

$$\hat{\mathbf{p}}=\underline{\mathbf{G}}^T\mathbf{w}, \tag{7}$$

where vector $\mathbf{w}$ is a dummy variable obtained by solving the linear system

$$\underline{\mathbf{D}}^{-1}(\underline{\mathbf{D}}\underline{\mathbf{G}}\underline{\mathbf{G}}^T\underline{\mathbf{D}} + \lambda\underline{\mathbf{I}})\underline{\mathbf{D}}^{-1}\mathbf{w} = \mathbf{d}, \tag{8}$$

where $\underline{\mathbf{I}}$ is an $N \times N$ identity matrix and $\underline{\mathbf{D}}$ is a diagonal normalizing matrix with elements:

$$d_{n,n} = \left[\sum_{m=1}^{M} g_{n,m}^2\right]^{-1/2}, \qquad n = 1, \ldots, N. \tag{9}$$

The purpose of normalization is to constrain the practical range of λ to the interval [0, 1].

The equivalent sources estimate $\hat{\mathbf{p}}$ provides an analytic harmonic function of the form

$$d(x, y, z) = \sum_{m=1}^{M} g(x - x_m, y - y_m, z - h)\hat{p}_m \tag{10}$$

that fits all observations if λ is equal to zero. When the data are corrupted with noise, an exact fit is not desirable. In this case, a value of λ greater than zero should be selected to produce misfits of the order of the noise amplitude in the data. The interpolated value d_k at position (x_k, y_k, z_k) is evaluated by equation (10) and can be written as a dot product

$$d_k = \mathbf{g}_{(k)}^T\hat{\mathbf{p}}, \tag{11}$$

or, using equation (7), as

$$d_k = \mathbf{g}_{(k)}^T\underline{\mathbf{G}}^T\mathbf{w}, \tag{12}$$

where $\mathbf{g}_{(k)}$ is a vector whose ith element is $g(x_k - x_i, y_k - y_i, z_k - h)$. The random to grid operation is realized by evaluation of equation (12) for a set of positions k situated on a regular grid.

Theoretically, the equivalent layer does not have to be at a constant depth. However, assuming equivalent layers at different depths will degrade the method's efficiency and make it less operational because the user will have to decide about the depth of the equivalent layer within each subarea corresponding to different subsets of the whole set of observations. The (constant) depth of the equivalent layer should not be smaller than 2.5 times the spacing between data points, otherwise aliasing may occur (Dampney, 1969). Particularly, in aeromagnetic and marine surveys, where the spacing between flight lines and ship tracks, respectively, may be substantially greater than the spacing between stations along a flight line (or track), the use of a shallow equivalent layer will produce aliasing in the interpolated data in the direction perpendicular to the flight lines (or tracks).

COMPARISON USING SYNTHETIC DATA

In this section, we simulate an aeromagnetic survey by computing the total-field anomaly caused by a vertical prism at stations regularly spaced along seven flight lines. The distances between the stations and the flight lines are 0.86 km and 8.6 km, respectively. These data were interpolated by the MCM and ELM producing a regular grid with a spacing of 2 km in both north-south and east-west directions. The theoretical anomaly is also obtained at points of this grid and, for each interpolation method, the difference between the true and interpolated anomalies is obtained at each grid point. In all tests, the prism magnetization was chosen to produce a maximum observed anomaly amplitude of 100 nT (in absolute value). In addition, a 15 km deep equivalent layer was employed, and λ was set to zero because the data are noise-free.

Undersampled anomaly flanks

Figure 1a shows the total-field anomaly produced by a cube whose plan view is shown in thick line. Its top is 8 km deep. The simulated flight lines are north-south and are also shown together with the stations positions. These data were interpolated by the ELM and MCM. The interpolating grid is indicated by tick marks at the figure borders. Figures 1b and 1c show the residuals (theoretical minus interpolated anomalies) associated with the ELM and MCM, respectively. In Figure 1b, the overall residual is smaller than 2 nT in absolute value. Only in a small area, close to the anomaly peak, is the residual greater than 2 nT. On the other hand, in Figure 1c, there are important areas with residuals greater than 2 nT and, close to the prism eastern and western borders, they exceed 4 nT and 6 nT, respectively. Other tests were performed placing the prism at different depths (from 5 km to 25 km at intervals of 1 km). For each test, the residual quadratic norm (square root of the sum of squared residuals at each grid point) was computed for each method and the results are displayed in Figure 1d. For both methods the residual norm decreases with the prism depth to the top because the anomaly becomes smoother. In addition, the ELM always produces a smaller residual norm than the MCM.

Undersampled anomaly peak

This test is similar to the previous one, the only difference being a westward shift in the prism position so that the anomaly peak is now located between two flight lines (Figure 2a). The residuals associated with the ELM and MCM are shown in Figures 2b and 2c. The ELM produces a maximum residual of about 4 nT at the anomaly peak while the MCM presents an 8 nT residual at the same point, indicating a better recovery of the anomaly peak by the ELM. In addition, the gradients to the north and to the south of the anomaly peak are better resolved by the ELM, producing a residual of about 2 nT as compared with 4 nT produced by the MCM. Figure 2d shows the residual quadratic norm as a function of the prism depth to the top. As in the previous case, the residual norm associated with the ELM is always smaller compared to the MCM.

Survey flown at different heights

The prism and survey layout (Figure 3a) are identical to those shown in the first test except that the observation points located in the northern half of the figure are 500 m below those in the southern half. The total-field anomaly is shown in Figure 3a which denotes, along the central flight line, a tenuous difference between the anomaly gradients in the northern and southern parts.

In interpolating these data by the ELM, all interpolated values were obtained at the level of the observation points

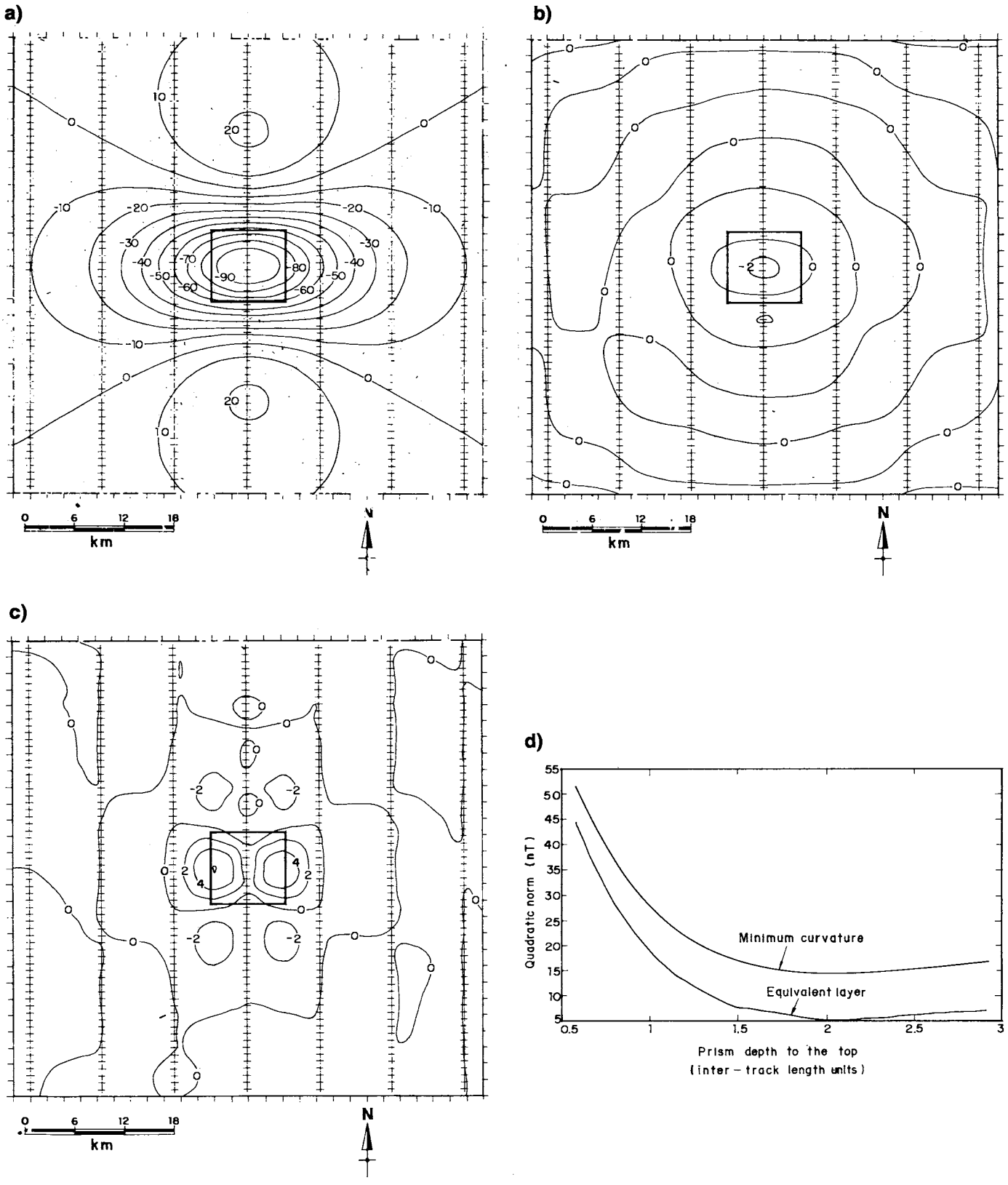

FIG. 1. Undersampled anomaly flanks. (a) Total-field anomaly and flight lines with the position of stations. Tick marks at the borders indicate the interpolation grid. Contour interval: 10 nT. (b) Residual between the theoretical anomaly in (a) and the interpolated anomaly using the ELM. Contour interval: 2 nT. (c) Residual associated with the MCM. Contour interval: 2 nT. (d) Residual quadratic norm for both interpolation methods as a function of the prism depth to the top.

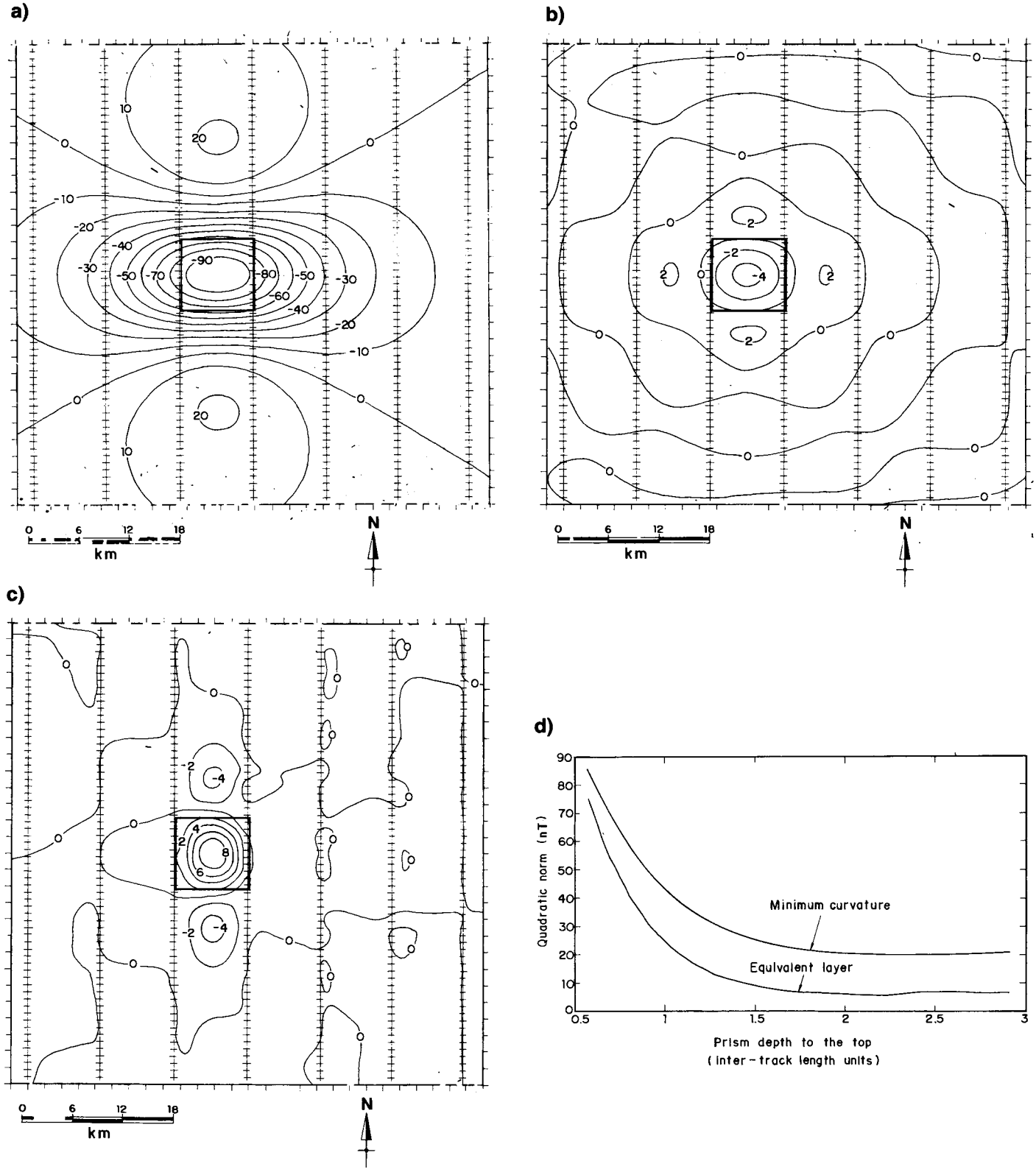

FIG. 2. Undersampled anomaly peak. (a) Total-field anomaly and flight lines with the position of stations. Tick marks at the borders indicate the interpolation grid. Contour interval: 10 nT. (b) Residual between the theoretical anomaly in (a) and the interpolated anomaly using the ELM. Contour interval: 2 nT. (c) Residual associated with the MCM. Contour interval: 2 nT. (d) Residual quadratic norm for both interpolation methods as a function of the prism depth to the top.

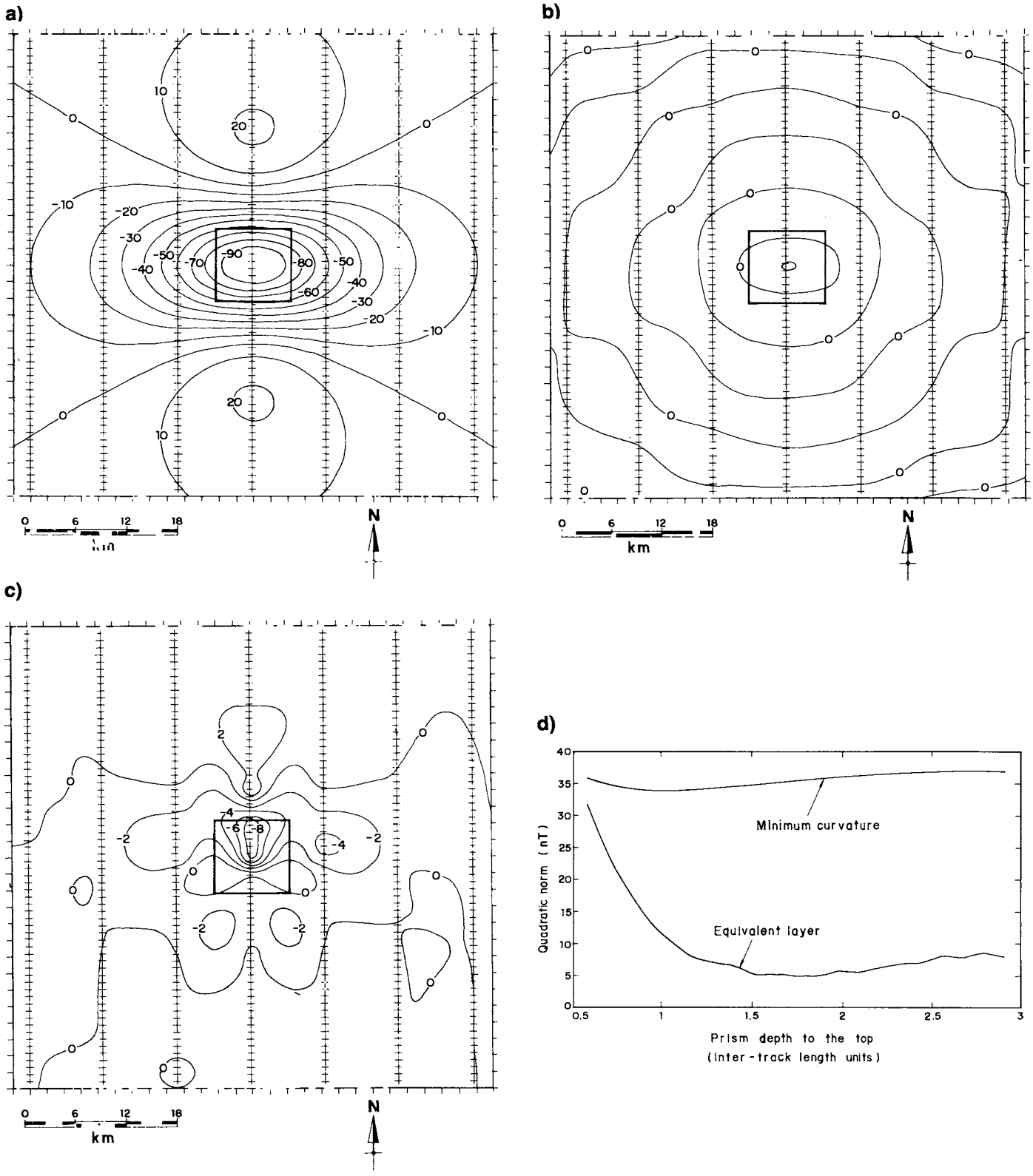

FIG. 3. Survey flown at different heights. (a) Total-field anomaly and flight lines with the position of stations. Tick marks at the borders indicate the interpolation grid. Contour interval: 10 nT. (b) Residual between the theoretical anomaly in (a) and the interpolated anomaly using the ELM. Contour interval: 2 nT. (c) Residual associated with the MCM. Contour interval: 2 nT. (d) Residual quadratic norm for both interpolation methods as a function of the prism depth to the top.

located in the northern half, that is, 500 m above the z-axis origin. The theoretical anomaly at this level was also computed to produce the residual maps associated with the ELM and MCM that are exhibited in Figures 3b and 3c, respectively. In Figure 3b, the residuals are as low as those obtained in the first test where the data were collected at the same level. In contrast, in Figure 3c, the residuals on the northern side of the anomaly minimum have high absolute values. This occurred because the MCM is a 2-D interpolation method and cannot take into account variations in the vertical coordinates of the observation points. Figure 3d shows the residual quadratic norm for both methods as a function of the prism depth to the top. In this case, the MCM produces a virtually constant residual norm of about 35 nT regardless of the prism depth. The ELM, as in the previous tests, produces smaller residual norms than the MCM regardless of the prism depth.

Elongated anomaly

In this test, we simulate a magnetic lineament by generating the total-field anomaly (Figure 4a) caused by a vertical, 8-km thick prism with horizontal dimensions of 4 km × 34 km and depth to the top at 8 km. Figures 4b and 4c show the total-field anomalies interpolated by the ELM and MCM, respectively. The ELM reproduced the anomaly linear character with great precision, but the MCM produced oscillations around the flight lines, destroying the anomaly linear aspect. Depending on the prism depth to the top (less than 6 km in this case), these oscillations may be so severe that the maximum amplitude contour (in absolute value) breaks into small circles around the flight lines, suggesting erroneously that the source top consists of several disjoint bodies. Figures 4d and 4e show the residuals associated with the ELM and MCM, respectively. Figure 4f displays the residual quadratic norm for both interpolation methods as a function of the source depth to the top. As in all previous tests, the ELM produces smaller residuals than the MCM regardless of the source depth.

CONCLUSIONS

Current interpretation methods use smoothness and continuity of the interpolating function to constrain the solution of the interpolation problem. The ELM is an interpolation method for potential-field data which, besides smoothness and continuity, introduces the constraint that the interpolating function must be harmonic.

A comparison between the ELM and the MCM indicates that, when the anomaly peak or flank is undersampled, the ELM performs better. In addition, the ELM does not produce the herringbone type anomalies associated with

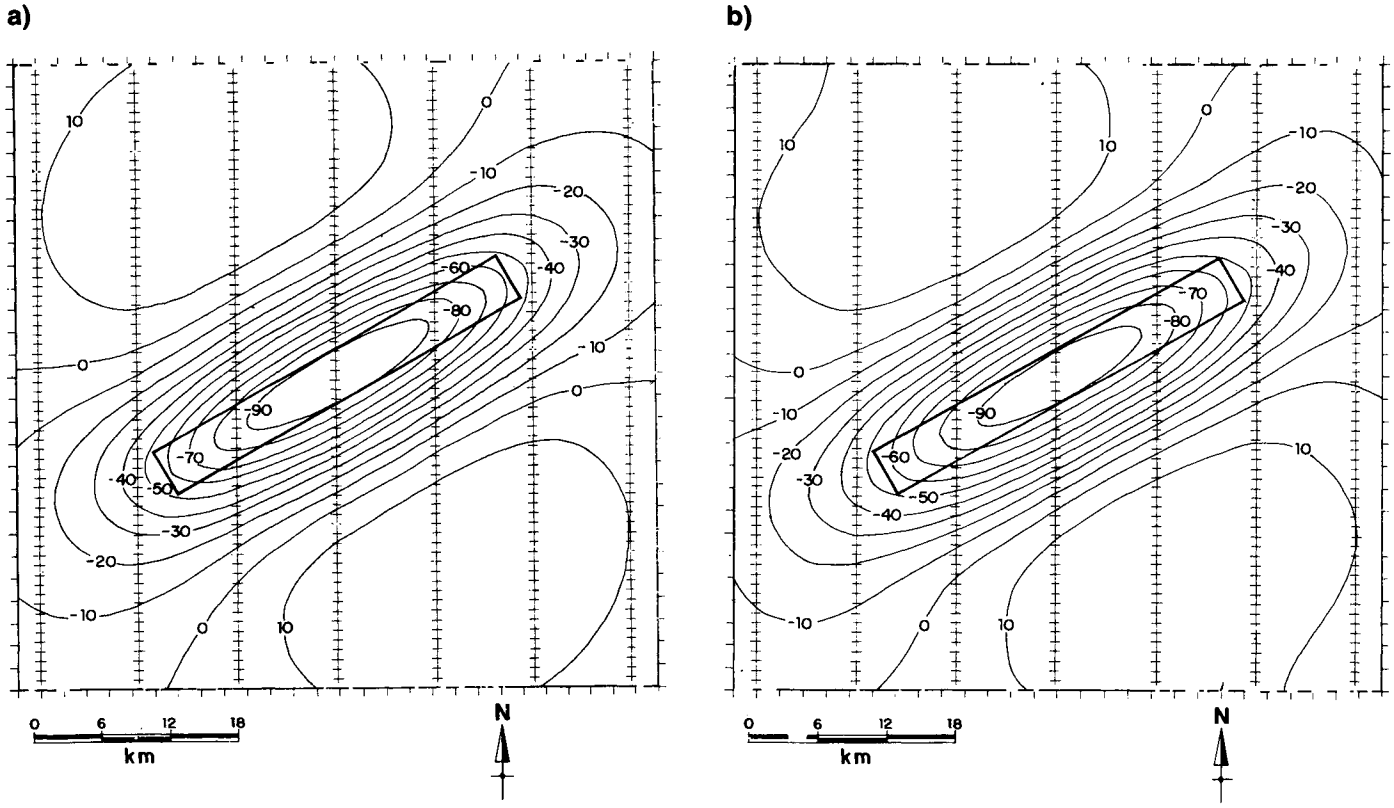

FIG. 4. Elongated anomaly. (a) Total-field anomaly and flight lines with the position of stations. Tick marks at the borders indicate the interpolation grid. Contour interval: 10 nT. (b) Interpolated anomaly using the ELM. Contour interval: 10 nT. (c) Interpolated anomaly using the MCM. Contour interval: 10 nT. (d) Residual between the theoretical anomaly in (a) and the interpolated anomaly using the ELM. Contour interval: 2 nT. (e) Residual associated with the MCM. Contour interval: 2 nT. (f) Residual quadratic norm for both interpolation methods as a function of the prism depth to the top.

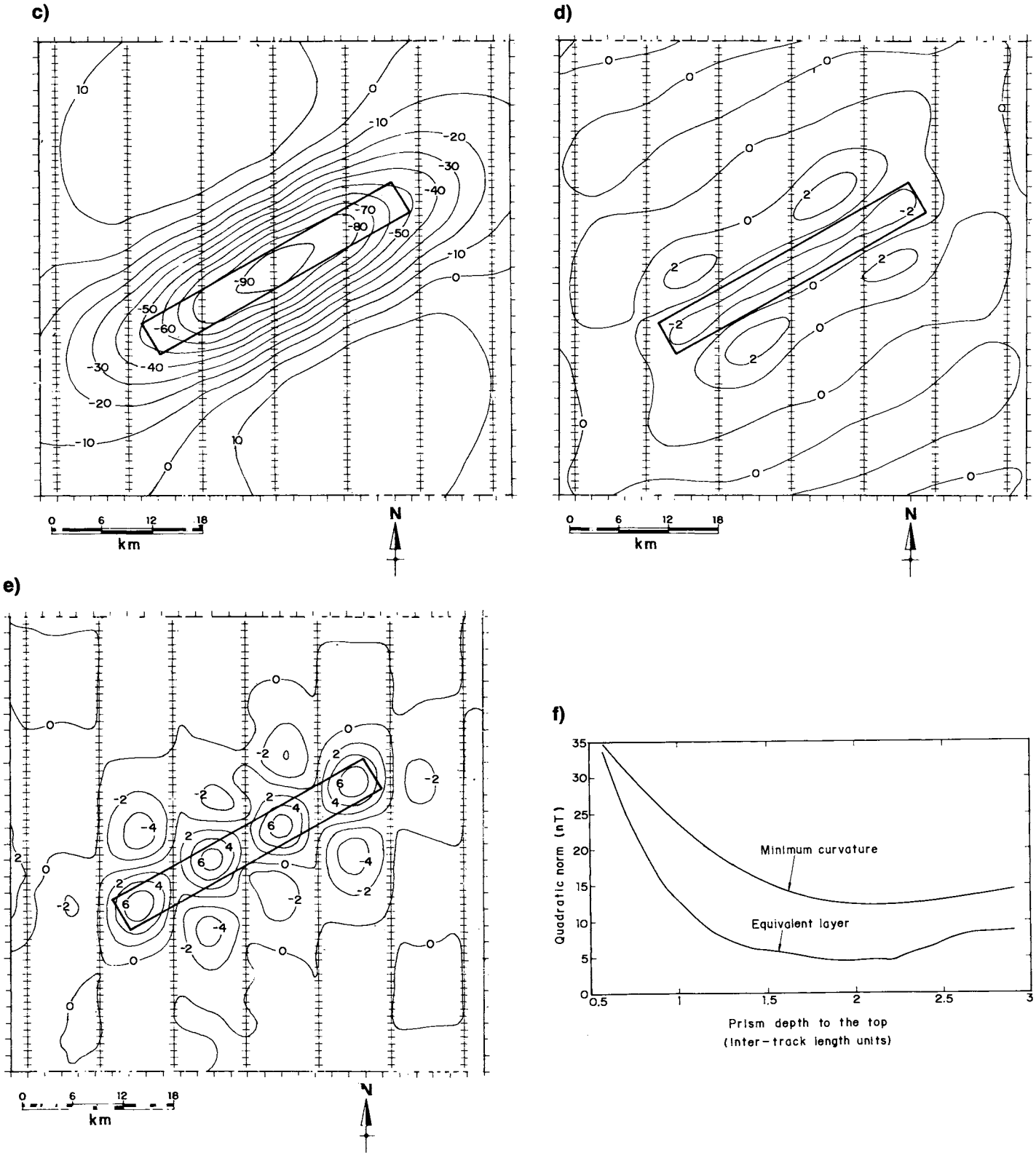

FIG. 4. (continued)

elongated anomalies which the MCM does. Finally, the ELM may be used to simultaneously interpolate and reduce data gathered at different heights to a common level.

ACKNOWLEDGMENTS

We thank Núcleo de Pesquisas em Geofísica de Petróleo (NPGP) and Conselho Nacional de Desenvolvimento Científico e Tecnológico (CNPq) for supporting this research.

REFERENCES

Bott, M. H. P., and Ingles, A., 1972, Matrix methods for joint interpretation of two-dimensional gravity and magnetic anomalies with application to the Iceland-Faeroe Ridge: Geophys. J. Roy. Astr. Soc., **30**, 55–67.

Braile, L. W., 1978, Comparison of four random to grid methods: Computers & Geosciences, **4**, 341–349.

Briggs, I. C., 1974, Machine contouring using minimum curvature: Geophysics, **39**, 39–48.

Cordell, L., 1992, A scattered equivalent-source method for interpolation and gridding of potential-field data in three dimensions: Geophysics, **57**, 629–636.

Dampney, C. N. G., 1969, The equivalent source technique: Geophysics, **34**, 39–53.

Emilia, D. A., 1973, Equivalent sources used as an analytic base for processing total magnetic field profiles: Geophysics, **38**, 339–348.

Franke, R., 1980, Scattered data interpolation: tests of some methods: Math. Comp., **38**, 181–200.

Gonzalez-Casanova, P., and Alvarez, R., 1985, Splines in geophysics: Geophysics, **50**, 2831–2848.

Gunn, P. J., 1975, Linear transformations of gravity and magnetic fields: Geophys. Prosp., **23**, 300–312.

La Porte, M., 1962, Elaboration rapide de cartes gravimetriques deduites de l'anomalie de Bouguer a l'aide d'une calculatrice electronique: Geophys. Prosp., **10**, 238–257.

Leão, J. W. D., and Silva, J. B. C., 1989, Discrete linear transformations of potential-field data: Geophysics, **54**, 497–507.

Mayhew, M. A., Johnson, B. D., and Langel, R. A., 1980, An equivalent-source model of the satellite-altitude magnetic anomaly field over Australia: Earth Plan. Sci. Lett., **51**, 189–198.

Mendonça, C. A., and Silva, J. B. C., 1994, The equivalent data concept applied to the interpolation of potential field data: Geophysics, **59**, 722–732.

Moritz, H., 1977, Least-squares collocation and the gravitational inverse problem: J. of Geophys., **43**, 153–162.

——— 1978, Least-squares collocation: Rev. Geophys. Space Phys., **16**, 421–430.

Morrison, F. F., and Douglas, B. C., 1984, A comparison of gravity prediction methods on actual and simulated data: Geophysics, **49**, 1774–1780.

Oldenburg, D. W., 1975, The inversion and interpretation of gravity anomalies: Geophysics, **39**, 526–536.

Shepard, D., 1969, A two-dimensional interpolation function for irregularly spaced data: Proc. 23rd Nat. Conf. ACM, 517–523.

Silva, J. B. C., 1986, Reduction to the pole as an inverse problem and its application to low-latitude anomalies: Geophysics, **51**, 369–382.